J. Phase Equilib. Diffus. (2020) 41:687–701
https://doi.org/10.1007/s11669-020-00837-x

Critical Assessment of the Al-Ti-Zr System

Z. Kahrobaee[1] · M. Palm[1]

Submitted: 28 July 2020 / Accepted: 8 September 2020 / Published online: 14 October 2020

Abstract Only within the last couple of years, complete isothermal sections for the Al-Ti-Zr system have been determined. Up to then there had been several investigations, but these were limited to the Ti-Zr and Ti-Al sides and the Ti- and Al corners of the system. Also recently the system has been evaluated by thermodynamic ab initio calculations and CALPHAD-type (CALculation of PHAse Diagrams) modelling. As Al-Ti-Zr alloys are of interest for a variety of applications and as the last assessment has been performed more than 15 years ago, this new critical evaluation of the existing literature about phase equilibria in the Al-Ti-Zr system has been performed.

Keywords assessment · crystal structures · modelling · phase equilibria

1 Introduction

In view of applications, different parts of the Al-Ti-Zr system are of interest and investigation of phase equilibria over the decades reflects these interests. With the development of Ti-base alloys, the extension of the homogeneity ranges of β(Ti,Zr) and α(Ti,Zr) within the ternary system in dependence of temperature have been investigated.[1–3] In the Al corner of the system precipitation of $(Ti,Zr)Al_3$ has been investigated for strengthening Al alloys at higher temperatures[4–7] and for grain refining.[8–10] As ductility may improve if instead of tetragonal $TiAl_3$ ($D0_{22}$) or $ZrAl_3$ ($D0_{23}$) metastable $(Ti,Zr)Al_3$ with cubic $L1_2$ structure forms, quite some effort has been spent on establishing phase stability in the Al-rich part of the system.[11–17] With the industrialisation of γ TiAl based alloys, phase equilibria among the Ti-Al based phases in this system came into focus.[18–23] While all these activities were limited to specific parts of the system, studies of full isothermal sections have been performed only very recently.[24,25]

Though of some practical importance, experimental difficulties in investigating Ti-Al(-X) systems at high temperatures make the determination of phase equilibria difficult. High susceptibility to impurities, specifically oxygen, which can have a pronounced effect on phase equilibria, reactions of melts with crucibles or preferential evaporation of Al are some of these problems.[26,27] The addition of Zr does not improve things, as it is also highly susceptible to oxygen uptake and because of its high melting point and low diffusivity, quite long annealing times are necessary to attain equilibrium even at high temperatures.[24,25] And the fact that even "high-purity" Zr contains comparable high amounts of impurities,[18,28] specifically Hf, is most of the time neglected.

The key for any aimed alloy development is a sound knowledge of phase equilibria in dependence of temperature and composition. In this regard, assessments play an important role as they collect all the available evidence and critically evaluate it. This is specifically true for the Al-Ti-Zr system, where until recently only scattered information had been available. The current work continues previous assessments by Ansara et al.[29] and Tretyachenko,[30] which have been performed in the framework of MSIT, the Materials Science International Team. The

✉ Z. Kahrobaee
z.kahrobaee@mpie.de

M. Palm
palm@mpie.de

[1] Max-Planck-Institut für Eisenforschung GmbH, Düsseldorf, Germany

activities of MSIT are inextricably associated with Günter Effenberg and his awareness of the importance of phase diagrams, thermodynamic and crystallographic data. This assessment is dedicated in memory of him.

2 Binary Systems

The binary Al-Zr system is accepted from (Ref 31). The different assessments of the Al-Zr system[31–33] and the thermodynamic modelling[34–36] are in good agreement with each other. According to them, ten stable intermetallic phases, all with restricted homogeneity ranges, exist: Zr_3Al, Zr_2Al, Zr_5Al_3, Zr_3Al_2, Zr_4Al_3, Zr_5Al_4, ZrAl, Zr_2Al_3, $ZrAl_2$, and $ZrAl_3$. Their crystallographic structures, lattice parameters and stability ranges are listed in Table 1. For $ZrAl_3$ it has been shown more recently that the phase forms by the peritectic reaction $L + ZrAl_2 \leftrightarrow ZrAl_3$[37] in agreement with a previous modelling,[32] rather than being a congruent melting compound.[31,33] The lower stability of the phases Zr_5Al_3 and Zr_5Al_4 and the upper stability of Zr_3Al_2 are uncertain.[31] Also the liquidus and solidus of β(Zr) have not been precisely determined, while the β(Zr)/β(Zr) + Zr_3Al and β(Zr)/β(Zr) + α(Zr) phase boundaries were determined in (Ref 38). The Ti-Zr system, which is accepted from Malfliet et al. (Ref 39), shows complete miscibility in the liquid and in the solid. The Ti-Al system has been assessed more recently in (Ref 27,40,41). Here the version by (Ref 27) is accepted, as it seems to be the most comprehensive evaluation of experimental data. While no substantial new experimental results have become available since then, modelling may yield some insight in two existing controversies about phase equilibria in the Ti-Al system.[42] The first one regards the possible B2 ordering in β(Ti). Wang et al. (Ref 43) combined ab initio calculations with CALPHAD modelling and showed that in the "pure" Ti-Al system no B2 ordering is observed. However, if substitutional vacancies and anti-site defects are taken into account in B2, then ordered β(Ti) is observed, thereby stabilising β(Ti) at higher Al contents. As a consequence, B2-ordered β(Ti) forms an equilibrium with α_2 Ti_3Al, whereby the homogeneity range of α(Ti) gets interrupted by the two invariant reactions β(Ti) + α(Ti) ↔ Ti_3Al at about 1200 ± 10 °C and β(Ti) + Ti_3Al ↔ α(Ti) at 1170 ± 10 °C.[43] As substitutional vacancies and anti-site defects have to be expected at the respective temperatures, it now becomes clear why, in contrast to experimental evidence, modelling of the "pure" Ti-Al system shows a continuous α(Ti) phase field.[43–48] Another open question is the transition from high-temperature $TiAl_3$ ($D0_{22}$) to the low-temperature $D0_{23}$-polymorph.[27] Recent density functional theory (DFT) calculations by Fang and Fan (Ref 49) showed that a series of intermediate stacking configurations of high stability exist. As even annealing for long time at intermediate temperatures may not equilibrate these "wrong" stacking, it becomes clear why $TiAl_3$ compounds of varying stacking sequences have been observed in dependence on individual experimental conditions.[50] Therefore also the recent update of the system[42] shows only the presence of the two polymorphs $TiAl_3$ (h) and $TiAl_3$ (l), but no transformation temperature.

3 Phases

Some of the binary phases show large solid solubility ranges for the third element and two ternary compounds, Ti_2AlZr[51–53] and Zr_2TiAl,[54] have been reported which actually could be ordered structures within the wide homogeneity range of β(Ti,Zr).

Addition of Zr to Ti or Ti to Zr stabilizes β with respect to α, i.e. in both cases the α/β transformation temperature is lowered.[55,56] Within the Al-Ti-Zr system β(Ti,Zr) encompasses a wide range of compositions. At high temperatures it includes the stoichiometric compositions Ti_2AlZr and Zr_2TiAl, for which both specific crystallographic structures have been reported (Table 1).

Al-rich samples of β(Ti,Zr) annealed for 168 h at 900 °C showed B2-ordering.[57] In an as-cast alloy of stoichiometric composition, the two phases Ti_2AlZr and Zr_5Al_3 were observed.[52] In the as-cast condition Ti_2AlZr showed the $D0_{19}$ structure, space group *P6₃/mmc*, while after annealing at 1200 °C for 30 min and also after subsequent ageing at 500 °C for 100 h or at 700 °C for 24 h single-phase B2-ordered β(Ti,Zr) was obtained.[52] Mechanical deformation lead to the formation of orthorhombic martensite.[52,58] B2 ordering was also reported for Al-rich β(Ti,Zr) synthesised from hydrides at 1000 °C.[59] Contrary to these observations, Ti_2AlZr with $D0_{19}$ structure was also observed after annealing an arc-melted button of the stoichiometric composition at 1000 °C for 720 h.[51] This is in agreement with ab initio calculations, which predicted that Ti_2AlZr will have the $D0_{19}$ structure.[53,60,61] However, quenching or deformation of Ti-rich compositions of β(Ti,Zr) may lead to formation the hexagonal ω phase and orthorhombic α″ and hexagonal α′ martensite[52,53,56,58] like in many other Ti-based alloys, e.g. in the Ti-Al-Nb system. However, details how the formation of the individual crystallographic structures depends on composition and quenching conditions still have to be established. The site occupation within the B2-ordered phase has been modelled by ab initio calculations.[62] Interdiffusion coefficients for Ti-rich β(Ti,Zr) at 1000 °C and 1200 °C have been determined in (Ref 63).

Table 1 Crystallographic data of solid phases

Phase/(Strukturbericht designation), Temperature range, °C	Pearson symbol/space group/prototype	Lattice parameters, pm	Comments/references
(Al), (*A1*), < 660.452	*cF4*	a = 404.96	Pure Al at 25 °C[80]
	Fm $\bar{3}$*m*		
	Cu		
β(Ti), (*A2*), < 1670-882	*cI2*	a = 330.65	(Ref 80)
	Im $\bar{3}$*m*	a = 322.8	Dissolves 44.6 at.% Al at 1491 °C[27]
	W	35.1 at.% Ti, 23.7 at.% Al, 41.2 at.% Zr[24]	Dissolves ~ 25 at.% Al at ~ 25 at.% Zr, ~ 50 at.% Ti at 1000 °C[24]
α(Ti), (*A3*), 1491-1120 and < 1170	*hP2*	a = 295.06	Pure Ti at 25 °C[80]
	P6$_3$*/mmc*	c = 468.35	Dissolves 50.5 at.% Al at 1456 °C[27]
	Mg		Dissolves 5.8 at.% Zr at 1000 °C[24]
α_2Ti_3Al, (*D0*$_{19}$), < 1200	*hP8*	a = 576.5	<20-38.5 at.% Al[27]
	P6$_3$*/mmc*	c = 462.5	Dissolves ~ 20 at.% Zr at 1000 °C[24]
	Ni_3Sn	[87]	
		a = 578.3	
		c = 466.7	
		52.1 at.% Ti, 28.0 at.% Al, 19.9 at.% Zr[24]	
γ TiAl, (*L1*$_0$), < 1456	*tP4*	a = 400.0	46.5- ~ 73 at.% Al[27]
	P$_4$*/mmm*	c = 407.5	Dissolves ~ 7.9 at.% Zr at 1000 °C[24]
	AuCu	at 50 at.% Al	Dissolves ~ 13 at.% Zr at 1274 °C[18]
		[88]	
		a = 408.0	
		c = 408.7	
		~42 at.% Ti, ~ 47 at.% Al, ~ 11 at.% Zr[71]	
		a = 397.4	
		c = 407.2	
		41.5 at.% Ti, 50.6 at.% Al, 7.9 at.% Zr[24]	
$TiAl_2$, < 1215	*tI24*	a = 397.1	65.5-67.0 at.% Al[27]
	I4$_1$*/amd*	c = 2431.2	Dissolves 11.5 at.% Zr at 1000 °C[24]
	$HfGa_2$	[89]	Dissolves 11.2 at.% Zr at 800 °C[25]
1d-APS (Ti_5Al_{11},Ti_2Al_5)	tetragonal ordered superstructures of AuCu	a = 392.30	for Ti_5Al_{11} (*I4/mmm, tI16*, $ZrAl_3$[91])
one-dimensional antiphase domain structures which form on cooling in Al-rich TiAl		c/4 = 413.37	for Ti_2Al_5 (*P4/mmm, tP28*, Ti_2Al_5[92])
		[90]	
		a = 390.53	
		c/7 = 417.03	
		[90]	

Table 1 continued

Phase/(Strukturbericht designation), Temperature range, °C	Pearson symbol/space group/prototype	Lattice parameters, pm	Comments/references
$TiAl_3$ (h), ($D0_{22}$), 1387-?	*tI8*	a = 384.9	74.2-75.5 at.% Al[27,42]
	I4/mmm	c = 861.0	
	$TiAl_3$ (h)	[93,94]	
$TiAl_3$ (l), ($D0_{23}$), ?	*tI32*	a = 387.7	74.2-75.5 at.% Al[27,42]
	I4/mmm	c = 3383.2	Dissolves 7.5 at.% Zr at 1000 °C[24]
	$TiAl_3$ (l)	[93,94]	
β(Zr), (*A2*), < 1855-863	*cI2*	a = 360.90	(Ref 80)
	Im $\bar{3}m$	[31]	Dissolves 26 at.% Al at 1350 °C[32]
	W		
α(Zr), (*A3*), < 863	*hP2*	a = 323.16	Pure (αZr) at 25 °C[80]
	$P6_3/mmc$	c = 514.75	Dissolves 8.3 at.% Al at 910 °C[38]
	Mg	[31]	
Zr_3Al, ($L1_2$), < 1019 ± 2	*cP4*	a = 437.3	(Ref 38)
	Pm $\bar{3}m$	[31]	
	Cu_3Au		
Zr_2Al, ($B8_2$), < 1215 ± 10	*hP6*	a = 489.39 ± 0.05	(Ref 38)
	$P6_3/mmc$	c = 592.83 ± 0.05	Dissolves 10.6 at.% Ti at 1000 °C[24]
	Ni_2In	[31]	Dissolves 13.8 at.% Ti at 800 °C[25]
Zr_5Al_3, ($D8_m$), < 1400-1000	*tI32*	a = 1104.4	(Ref 31,95)
	I4/mcm	c = 539.1	
	W_5Si_3	[31]	
Zr_5Al_3, ($D8_8$), (< 1000?)	*hP16*	a = 817.4	(Ref 69,96)
	$P6_3/mcm$	c = 569.8	Dissolves 32.0 at.% Ti at 1000 °C[24]
	Mn_5Si_3	[31]	
		a = 821.7	
		c = 570.4	
		30.5 at.% Ti, 39.2 at.% Al, 30.3 at.% Zr[24]	
Zr_3Al_2, < 1480	*tP20*	a = 763.0 ± 0.01	(Ref 31)
	$P4_2/mnm$	c = 699.8 ± 0.01	Dissolves 14.4 at.% Ti at 800 °C[25]
	Zr_3Al_2	[31]	
Zr_4Al_3, < 1030	*hP7*	a = 543.3 ± 0.2	(Ref 31)
	P6/mmm	c = 539.0 ± 0.2	Dissolves 5.6 at.% Ti at 1000 °C[24]
	Zr_4Al_3	[31]	Dissolves 13.5 at.% Ti at 800 °C[25]
		a = 541.1	
		c = 535.4	
		5.6 at.% Ti, 43.4 at.% Al, 51.0 at.% Zr[24]	

Table 1 continued

Phase/(Strukturbericht designation), Temperature range, °C	Pearson symbol/space group/prototype	Lattice parameters, pm	Comments/references
Zr_5Al_4, < 1550- ~ 1120 (?)	*hP18* *P6$_3$/mcm* Ti_5Ga_4	a = 844.8 c = 580.5 [31]	(Ref 31,68)
ZrAl, (*B33*), < 1225 ± 25	*oC8* *Cmcm* CrB	a = 335.9 ± 0.1 b = 1088.7 ± 0.3 c = 427.4 ± 0.1 [31]	(Ref 31)
Zr_2Al_3, < 1572 ± 3	*oF40* *Fdd2* Zr_2Al_3	a = 960.1 ± 0.2 b = 1390.6 ± 0.2 c = 557.4 ± 0.2 [31]	(Ref 37) Dissolves 0.8 at.% Ti at 1000 °C[24] Dissolves 1.3 at.% Ti at 800 °C[25]
		a = 958.9 b = 1394.6 c = 557.8 0.3 at.% Ti, 59.8 at.% Al, 40.2 at.% Zr[24]	
$ZrAl_2$, (*C14*), < 1624	*hP12* *P6$_3$/mmc* $MgZn_2$	a = 528.24 ± 0.05 c = 874.82 ± 0.05 [31]	(Ref 37) Dissolves 8.7 at.% Ti at 1000 °C[24]
		a = 527.3 c = 882.7 8.7 at.% Ti, 60.1 at.% Al, 31.2 at.% Zr[24]	
$ZrAl_3$, ($D0_{23}$), < 1579 ± 3	*tI16* *I4/mmm* $ZrAl_3$	a = 399.93 ± 0.05 c = 1728.3 ± 0.2[31]	(Ref 37) Dissolves about 12 at.% Ti at 1000 °C[24]
Ti_2AlZr, (*B2*)	*cP2* *Pm* $\bar{3}$*m* CsCl	a = 333(6)[52]	After annealing the stoichiometric composition at 1200 °C[52]
Ti_2AlZr, ($D0_{19}$)	*hP8* *P6$_3$/mmc* Ni_3Sn	a = 596.1 ± 0.1 c = 479.3 ± 0.1 [51]	After annealing the stoichiometric composition at 1000 °C[51]
Zr_2TiAl, ($L2_1$)	*cF16* *Fm* $\bar{3}$*m* $AlCu_2Mn$	a = 684.00 [54]	After annealing the stoichiometric composition at 1000 or 1050 °C[54]

A phase Zr_2AlTi with cubic $L2_1$ structure, space group $Fm\bar{3}m$ was found in an alloy of stoichiometric composition after annealing at 1050 °C for 720 h or 1000 °C for 480 h.[54] The analysed composition of Zr_2AlTi lies near or at the β(Ti,Zr)/β(Ti,Zr) + $(Zr,Ti)_5Al_3$ phase boundary.[24,64] That Zr_2AlTi was accompanied by two other phases, of which one could be $(Zr,Ti)_5Al_3$ or $(Zr,Ti)_2Al$ according to X-ray diffraction (XRD) and analysed composition,[54] may indicate that also this structure may result from ordering within β(Ti,Zr).

All phases originating in the binary Ti-Al system show a marked solid solubility for Zr (Table 1). At 1000 °C 6 at.% Zr in α(Ti,Zr), 20 at.% Zr in Ti_3Al, 8 at.% Zr in TiAl, 12 at.% Zr in $TiAl_2$ and 7.5 at.% Zr in $TiAl_3$ may dissolve.[24] The solid solubility in all phases seems to increase with increasing temperature, e.g. at 1274 °C about 13 at.% Zr may dissolve in TiAl.[18] For the site occupation of Zr in TiAl a strong preference for Ti sites was found.[18,20–22,65,66] Also in Ti_3Al Zr substitutes for Ti.[22,65,66] It was also found that the temperature of the α(Ti,Zr)/Ti_3Al phase boundary is only slightly raised by the addition of Zr.[3]

The change from $TiAl_3$ with $D0_{22}$-structure to $ZrAl_3$ ($D0_{23}$-structure) along $(Ti,Zr)Al_3$ in dependence of composition and temperature was investigated by high-temperature XRD.[12] Lattice constants for $(Ti,Zr)Al_3$ with $D0_{22}$- and $D0_{23}$-structure have been determined in (Ref 4,6,12,59) and for metastable $L1_2$ in (Ref 7,11,13,15,16). The formation of metastable $(Ti,Zr)Al_3$ with $L2_1$-structure in Al has been investigated in (Ref 17) and transformation to stable $D0_{23}$ during aging between 450 and 600 °C was studied by transmission electron microscopy (TEM).[14]

Also, most phases originating in the binary Zr-Al system show a marked solid solubility for Ti (Table 1). Solid solubilities of about 12 at.% Ti in $ZrAl_3$, 9 at.% Ti in $ZrAl_2$, and even 32 at.% Ti in Zr_5Al_3 at 1000 °C[24] and about 14 at.% Ti in Zr_4Al_3, Zr_3Al_2 and Zr_2Al at 800 °C have been reported.[25]

4 Isothermal Section at 1000 °C

Most data are available for 1000 °C and the most comprehensive investigation was performed by (Ref 24), who determined a complete isothermal section (Fig. 1). More than 38 alloys of about 5 grams each were produced by arc-melting. As the weight loss during alloy production did not exceed 1%, nominal compositions have been considered as ultimate alloy compositions. Heat-treatments were performed at 1000 °C for 1440 h for samples encapsulated in quartz tubes back-filled with Ar followed by water quenching. Samples were examined by metallography, XRD and electron probe microanalysis (EPMA). Compositions of coexisting phases were established by an average of five EPMA measurements. The standard deviations of the measured concentrations are ± 0.6 at.% and the total mass of Al, Zr, and Ti was in the range of 97-103%. Figure 1 shows the established isotherm from (Ref 24). While no ternary phases were detected, most binary phases show marked solid solubility ranges for the third component. It is noted that phase boundaries do not match those currently accepted for Ti-Al[27] and that some phase boundaries are not in accordance with thermodynamic rules applying to isothermal sections.[67] Extrapolation of the phase boundaries from the ternary system onto the binary Al-Zr system shows that apparently the "line compounds" Zr_5Al_3 and $ZrAl_2$ have some marked solid solubility ranges in the binary. The phase Zr_3Al, which should be stable at 1000 °C (Table 1), has not been detected in (Ref 24). As the solid solubility for Ti in this phase could be very small, it may not have been observed, because no alloy of appropriate composition has been investigated. The phase Zr_5Al_4, which might be stable at 1000 °C,[31] has also not been detected in (Ref 24). This is in line with an investigation of the Fe-Al-Zr system, which showed that this phase may only become stable above ~ 1120 °C.[68] For a discussion, whether Zr_5Al_3 with the Mn_5Si_3-type crystal structure is stable in the binary Al-Zr system or not see (Ref 69). However, it is clear that impurities and third alloying elements stabilise the Mn_5Si_3-type structure in favour of W_5Si_3-type Zr_5Al_3, which might be the stable structure in binary Al-Zr at 1000 °C.[31] Therefore, it is plausible that [24] observed the Mn_5Si_3-type structure for $(Zr,Ti)_5Al_3$. The phase Ti_2Al_5 has by now been identified as a one-dimensional antiphase domain structure, which forms from TiAl that becomes supersaturated in Al on cooling.[27]

Among other investigations at this temperature, the homogeneity range of TiAl was studied on 24 different arc-melted alloys, heat-treated at 1000 °C for 10 h.[70] Phases were identified by XRD but no compositions of coexisting phases were established. The solid solubility for Zr in TiAl was found to be about 15 at.%, which is much higher than that reported in (Ref 24). Presumably—and as acknowledged by the authors—annealing times in (Ref 70) were too short for equilibrating TiAl. Therefore, alloys may have been supersaturated in Zr from the melting process at high temperatures and therefore the reported solid solubility may be too high. The solid solubility range of TiAl has also been examined on 21 alloys heat treated at 1000 °C for 168 h.[71] Phases were analysed by XRD and compositions of phases were established by EPMA, but only lattice constants for TiAl are given and compositions can only be read for TiAl from a figure. According to this study the maximum solid solubility for Zr in TiAl could be about 11 at.% at about 47 at.% Al. Also the presence of the three-

phase equilibria TiAl + Ti_3Al + ZrAl and TiAl + $ZrAl_2$ + ZrAl at 1000 °C is shown,[71] in contradiction to the results by (Ref 24). The occurrence of phase equilibria between TiAl and ZrAl seems unlikely, because the solid solubility for Ti in ZrAl is very limited compared to that in $ZrAl_2$ and Zr_5Al_3, which makes the presence of three-phase equilibria with the latter two phases more likely, as determined in (Ref 24) (Fig. 1 and 2). Two alloys investigated in (Ref 20) were single-phase TiAl after annealing at 1000 °C for 192 h, in accordance with (Ref 24). The width of the TiAl + Ti_3Al two-phase field at 1000 °C was studied in (Ref 19) on 10 alloys, which were equilibrated for 168 h. Phases were identified by XRD and for three alloys the compositions of the coexisting phases were established by EPMA. Compared to phase boundaries established in (Ref 24) and the current Ti-Al binary system, the results in (Ref 19) are somewhat shifted towards higher Ti contents by 2-3 at.%. The two-phase field was again studied in (Ref 23). Only one tie-line close to the Ti-Al binary system was established at 1000 °C, which fits very well with the binary.[27] The composition 50 ± 2 at.% Ti, 25 at.% Zr, 25 ± 2 at.% Al was found to be single-phase $D0_{19}$, the structure of Ti_3Al, after annealing at 1000 °C for 720 h.[51] Whether this means that Ti_3Al may have a larger solid solubility for Zr than ~ 20 at.%, as found in (Ref 24) or whether $D0_{19}$ forms on cooling at around 1000 °C from B2, as discussed before, cannot be settled based on the existing experimental evidence.

Vertical sections along Ti-14.9 at.% Al/Zr, Ti-25.3 at.% Al/Zr, and Ti-33.3 at.% Al/Zr were investigated in the 1960s by metallography, differential thermal analysis (DTA), and XRD and results were published in a series of overlapping papers.[55,64,72–75] At 1000 °C samples were annealed for 100 h and quenched in water. All values for phase boundaries taken from the figures are unreasonable at 1000 °C, as discussed later, except that for the α(Ti,Zr) + Ti_3Al/Ti_3Al phase boundary.[75] 9 diffusion couples prepared for a diffusion study in b.c.c. β(Ti,Zr) were apparently all single-phase β(Ti,Zr) after annealing for 48 h at 1000 °C,[63] in accordance with the composition range outlined in (Ref 24).

Finally, a ternary compound Zr_2TiAl with cubic $L2_1$-structure was identified in an alloy of appropriate composition that had been annealed for 480 h at 1000 °C and 720 h at 1050 °C.[54] As discussed before, it is assumed that the composition may lie within the extended single-phase region of β(Ti,Zr) and therefore ordering may occur on cooling.

Figure 1 shows the diagram established in (Ref 24) together with all other results from investigations at this temperature. Figure 2 shows the isothermal section as assessed from the results discussed above. It is based on the one established by (Ref 24) with the phase boundaries adjusted to match with those of the accepted binaries and to be in accordance with thermodynamic rules. A small phase field for Zr_3Al and respective tentative multi-phase equilibria have been added to comply with the accepted Al-Zr binary system. As it has not been settled yet, whether the compositions Ti_2AlZr and Zr_2TiAl are separate phases, or indicate B2-ordering at this temperature within Al-rich compositions of β(Ti,Zr),[52,57,59] an area where B2-ordering may occur has been outlined in Fig. 2.

5 Isothermal Section at 800 °C

A complete isothermal section at 800 °C[25] (Fig. 3) was determined by the same group that established the isotherm at 1000 °C using the same techniques as in (Ref 24), except that no XRD has been employed in (Ref 25). In addition, they employed a Ti/$TiAl_3$/Zr diffusion triple and this, like 12 alloys of fixed composition, was heat-treated for 2400 h at 800 °C. Again the isotherm contains some violations concerning thermodynamic rules and determined phase boundaries for the Ti-Al phases are not in good agreement with the accepted binary system,[27] particular in showing a much lower solid solubility of Al in α(Ti). Also at 800 °C no ternary phases are observed while all binary phases have considerable solid solubility ranges, with the exception of Zr_2Al_3 and ZrAl. The latter phase was not detected at all, presumably because of its limited homogeneity range in the ternary system. All ternary homogeneity ranges of the binary Zr-Al phases show a pronounced tendency for substitution of Zr by Ti, except $ZrAl_2$, which shows a pronounced tendency for substitution of Al by Ti (Fig. 3). Though a complete isotherm has been established, many three-phase fields have not been experimentally confirmed (dashed triangles in Fig. 3). Therefore it could be theoretically possible that instead of the two-phase equilibrium β(Ti,Zr) + Zr_4Al_3 the phases $ZrAl_2$ and Zr_3Al_2 are in equilibrium with each other. The solubility for Zr in $TiAl_2$ is 11.2 at.%, which is about the same value as at 1000 °C.[24] The solubility for Ti in Zr_2Al is 13.8 at.%, somewhat higher than at 1000 °C.[24] Solid solubilities of the third element in other binary phases could actually even be higher than indicated in Fig. 3, as the maxima shown there stem either from phase equilibria shown by dashed lines, i.e. experimentally not determined, or from evaluating the diffusion path in the diffusion triple. As the diffusion path will always cross two-phase fields, established compositions can be more or less close to the three-phase equilibrium and therefore do not correspond to a maximum solid solubility in a phase.

Otherwise, there are few other data available for this temperature, mostly for the Ti corner. The effect of Zr addition on the α(Ti,Zr)/α(Ti,Zr) + Ti_3Al phase boundary

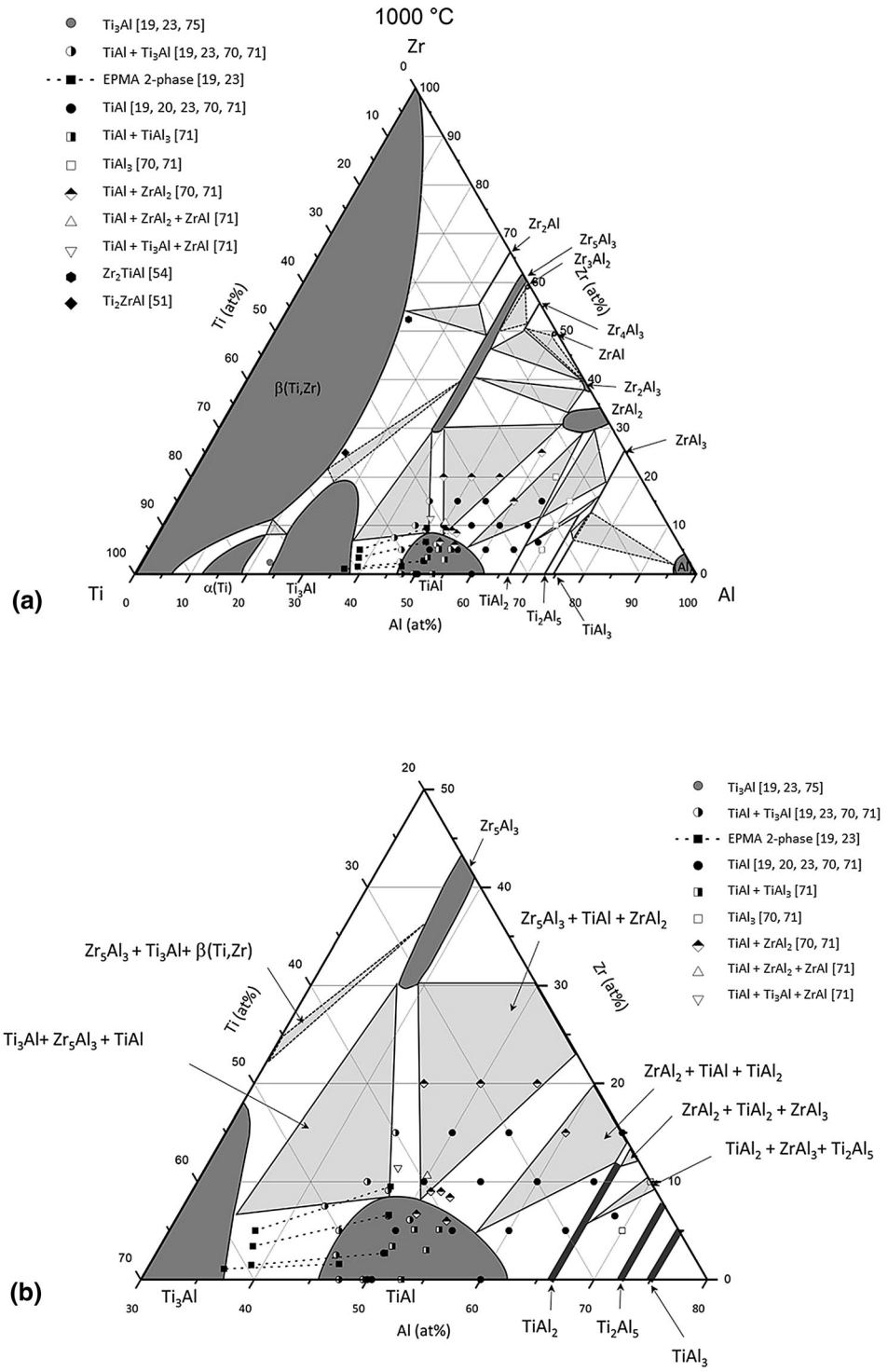

Fig. 1 (a) Isothermal section at 1000 °C according to [24] with additional experimental results from the literature. (b) Enlarged area from this figure showing phase equilibria and experimental results for TiAl in more detail

was investigated in (Ref 2) in the composition range Ti-(8-13)Al-(1-2)Zr at.%. Alloys were produced by arc-melting and rolled prior to annealing at 800 °C for 200 h under flowing Ar. Chemical analyses after heat treatment were in good agreement with the nominal compositions and the amount of oxygen was assumed to be 0.03 to 0.04 wt.%. By light microscopy it was established that all investigated alloys were single-phase α(Ti,Zr) at 800 °C. This shows that α(Ti,Zr) extends to somewhat more Zr-rich and markedly more Al-rich compositions than shown in Fig. 3, in good agreement with the accepted binary Ti-Al system.[27]

Quite a couple of vertical sections exist, which include results at 800 °C.[64,72–76] Though, all of them either

missed out some phases and/or phase equilibria, denote data points to other phase boundaries than those shown in Fig. 3 or are contradictory in itself (for a detailed discussion see section on Vertical Sections). However, as far as the Ti corner has been investigated, they are inline that α(Ti,Zr) extends further into the ternary system than shown in (Ref 25).

Four samples in the Al corner of compositions 0-15Ti-Al-5Zr (at.%) were investigated in (Ref 77). The samples were prepared by annealing pre-cursors pressed from elemental powders at 800 °C for 30 min. Samples were analysed by observations in a scanning electron microscope (SEM), XRD and electron-dispersive X-ray spectroscopy (EDS). All alloys consist of the two phases Al + (Zr,Ti)Al_3. According to the isothermal section by Lü et al., (Ref 25) the two Ti-rich compositions should show the three-phase equilibrium Al + (Zr,Ti)Al_3 + $TiAl_3$ at 800 °C (Fig. 3). One explanation for this discrepancy could be that the annealing time of 30 min was too short to attain equilibrium.

The isothermal section assessed here is shown in Fig. 4. It is based on the results by (Ref 25) with an increased solid solubility range for α(Ti,Zr), in agreement with (Ref 2) and the binary Al-Ti system. Phase boundaries have been adjusted to match with those of the accepted binaries and to be in accordance with thermodynamic rules.

6 Data at Temperatures Below 800 °C

As attaining thermodynamic equilibrium in Al-Ti-Zr alloys at low temperatures becomes more and more difficult, data on phase equilibria below 800 °C are scarce. The effect of Zr addition on the α(Ti,Zr)/α(Ti,Zr) + Ti_3Al phase boundary in the temperature range 500-700 °C is shown in (Ref 2), which also shows a partial isothermal section at 700 °C. The phase boundary matches well with the accepted binary.[27] From a series of 16 alloys equilibrated for 500 h at 700 °C, the phase boundaries of the two-phase field α(Ti,Zr) + Ti_3Al with up to 5 wt% Zr were determined.[75] Compared to the binary system, the two phase area widens by the addition of Zr, in line with the observation by (Ref 2). The α(Ti,Zr)/α(Ti,Zr) + Ti_3Al phase boundary was also studied at 600 °C by equilibrating alloys with 2, 6 and 10 at.% Zr for 400 h.[78] The extrapolated phase boundary matches well with the extrapolated

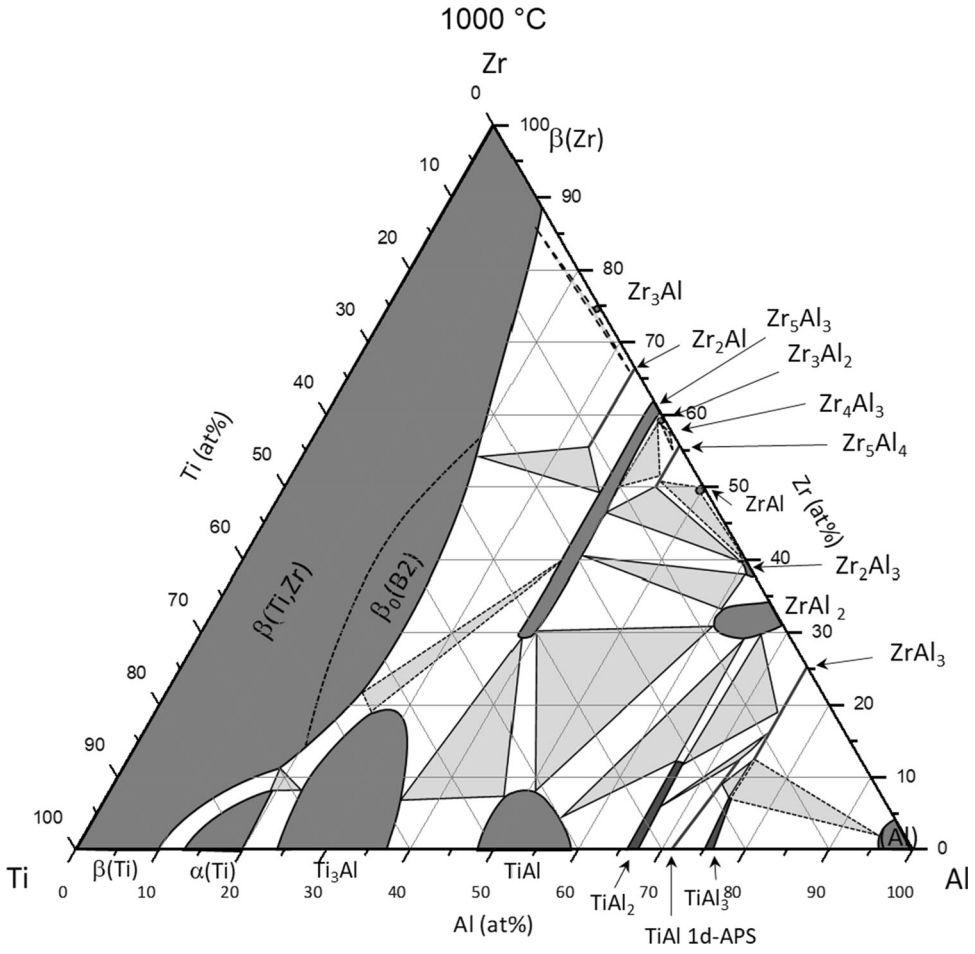

Fig. 2 Critically assessed isothermal section of the Al-Ti-Zr system at 1000 °C

one in the binary Al-Ti system.[27] A partial isothermal section of the Ti-corner at 500 °C showing the α(Ti,Zr) + Ti_3Al phase area is included in (Ref 75).

7 Data at Temperatures Above 1000 °C

Information above 1000 °C is limited to phase equilibria between the phases α(Ti,Zr), β(Ti,Zr) and TiAl. The phase relations between these phases have been studied by investigating alloys annealed at 1200 °C for 168 h and at 1300 °C for 24 h.[23] Heat treatments were carried out in quartz capsules, which are usually considered not to be any longer gas-tight at these temperatures. However, oxygen and nitrogen contents were below 400 (wt.) ppm after the heat treatments. Compositions of coexisting phases in the quenched samples were determined by EPMA by averaging data from 10 points. At 1200 °C the three-phase equilibrium α(Ti,Zr) + β(Ti,Zr) + TiAl could be determined, showing a maximum solid solubility of 5.1 at.% Zr in α(Ti,Zr). Though this tie-triangle was not measured directly at 1300 °C, the adjacent tie-lines suggest that the solubility for Zr in α(Ti,Zr) may only slightly increase up to about 5.5 at.% Zr at this temperature.

In the diffusion study of b.c.c. β(Ti,Zr),[63] 11 diffusion couples were annealed for 17 h at 1200 °C. All of them were single-phase β(Ti,Zr) after annealing, in accordance with the β(Ti,Zr)/β(Ti,Zr) + α(Ti,Zr) and β(Ti,Zr)/β(Ti,Zr) + TiAl phase boundaries determined by (Ref 23) for lower Zr contents.

An arc melted alloy of the composition Ti-24.8Al-24.9Zr at.% that was solution treated at 1200 °C for 30 min and water quenched, was found to be single-phase B2-ordered β(Ti,Zr) by TEM.[52] As no anti-phase domains were observed, the authors concluded that the alloy has been B2 at 1200 °C and did not undergo ordering at lower temperatures during quenching.

In a couple of early studies, the extension of the TiAl phase field at 1093 °C[79] and 1274 °C [18,28] was studied by metallography and XRD. At 1093 °C, 27 different alloys were heat treated for 36-39 h and air cooled.[79] The maximum solid solubility for Zr in TiAl was found to be about 8 at% at 1093 °C.[79] A first partial isothermal section for "1274 °C" was constructed from 19 alloys, which were actually heat treated between 1246 and 1379 °C for 24-39 h.[28] The partial isothermal section for 1274 °C was updated by 18 alloys, which were wrapped in Ta foil and encapsulated in quartz ampules for the heat treatments and which were quenched in brine after annealing for 24 h.[18] As the determined composition range for TiAl in the binary system is shifted markedly to higher Al contents compared to the currently accepted one,[27] the established solid solubility limit of about 13 at.% Zr in TiAl at 1274 °C[18] could be doubted. For establishing various vertical sections, quite a couple of alloys have been studied, which have been equilibrated at 1100 °C.[64,72,73,75] As discussed in more detail in the following section, these results are all considered to be questionable.

8 Vertical Sections

8.1 Sections Towards the Zr Corner

The vertical section Ti-14.9 at.% Al/Zr was investigated between 500 and 1100 °C by metallography of 19 different annealed alloys and thermal analysis.[72] Established phase boundaries do not match at 800 °C with the current knowledge of the binary Ti-Zr system or the ternary system (Fig. 4) with the sole exception of the β(Ti,Zr)/α(Ti,Zr) + β(Ti,Zr) phase boundary. Therefore, the location of the minimum in the α(Ti,Zr)/β(Ti,Zr) transformation temperature of about 660 °C and 65 wt% Zr may be doubtful. A comparable minimum was found in the vertical section Ti-25.3 at.% Al/Zr at about 515 °C and 70 wt% Zr.[55] In this study, the vertical section has been determined between 500 and 1900 °C by thermal analysis of 11 alloys and microstructural and XRD investigations of quenched alloys.[55] Beside determination of the solidus temperatures, phase boundaries of the α(Ti,Zr), α(Ti,Zr) + β(Ti,Zr), and β(Ti,Zr) phase fields were determined. The melting temperature determined for Zr (1850 °C) and the solidus temperature of Ti_3Al with 24.1 at.% Al (~ 1650 °C) are very close to the currently accepted values 1855 °C[80] and 1655 °C.[27] Therefore, remaining solidus and liquidus temperatures determined in (Ref 55) may be considered as relevant. Though the existence of the compound Ti_3Al has been realised in (Ref 55), the phase has not been included in the vertical section. Also, according to the isotherms at 800 °C and 1000 °C shown in Fig. 2 and 4, this vertical section should include phase equilibria with quite a number of other phases e.g. TiAl or $Zr(Al,Ti)_2$. As no other phases than α(Ti,Zr) and β(Ti,Zr) are shown in the section, solid phase equilibria from[55] are not further considered here. One more "tentative" section along Ti-33.3 at.% Al/Zr[64] was constructed from 20 samples annealed between 500 and 1100 °C, which were analyzed by metallography and partly by XRD, supplemented by data from thermal analysis. The section had been tentative, as many alloys underwent phase transformations during cooling and therefore phase equilibria at the annealing temperature were not clear. Again the section misses out phase equilibria with the phases originating in the Al-Zr binary system, with the exception of Zr_3Al, which according to this section would coexist

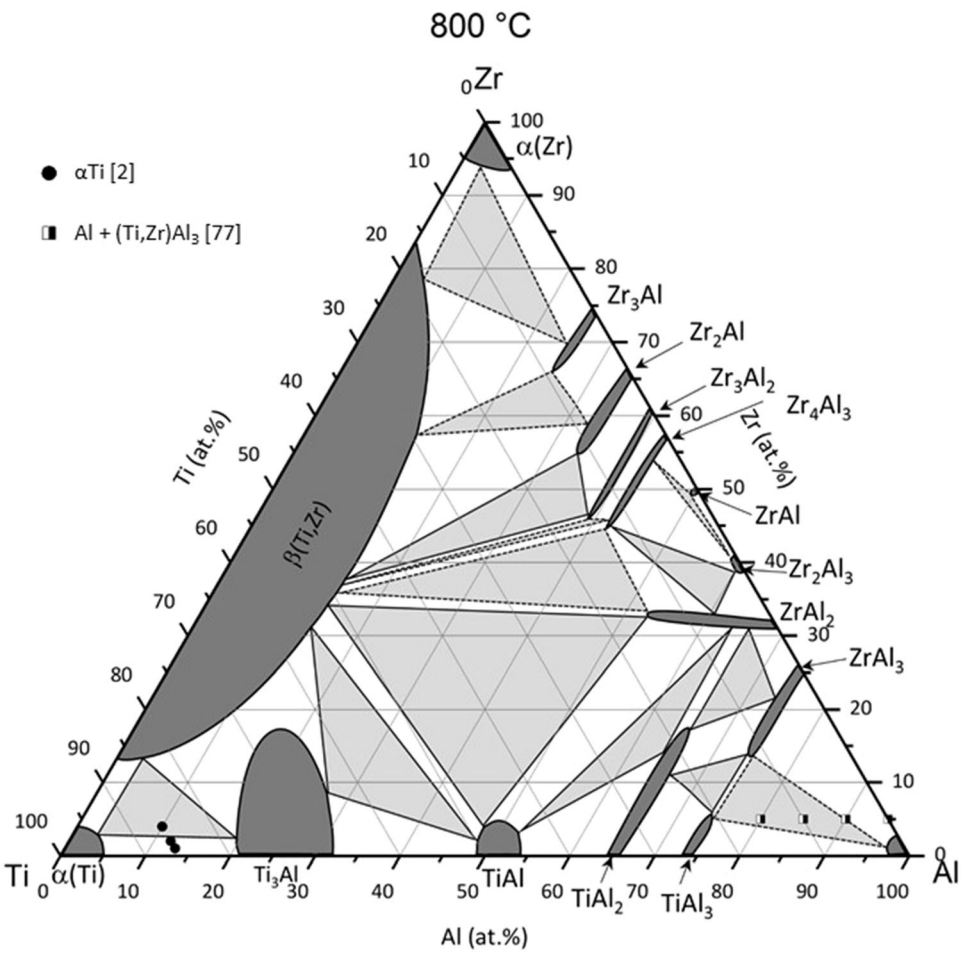

Fig. 3 Isothermal section at 800 °C according to (Ref 25) with additional experimental results from the literature

over a large composition range with α(Ti,Zr) and β(Ti,Zr).[64]

In the vertical sections Ti/Ti-49.4 at.% Zr containing 0, 6.9, and 9.6 at.% Al the phase boundaries for α(Ti,Zr) and β(Ti,Zr) between 600 and ~1100 °C were determined by metallography of annealed samples and additional dilatometry for the binary section.[76] All phase boundaries show a sharp increase in temperature between 0 and about 1 at.% Zr, e.g. about 45 K for α(Ti,Zr)/α(Ti,Zr) + β(Ti,Zr), and then temperatures decrease steadily to 49.4 at.% Zr. As far as temperatures can be read from the diagram, they seem not to match phase boundaries shown for 800 °C and 1000 °C in Fig. 2 and 4 and as a peak in temperature in the α(Ti,Zr) and β(Ti,Zr) phase boundaries is thermodynamically improbable, results of (Ref 76) are not further considered here.

8.2 Sections Towards the Al Corner

Based on metallography on heat treated samples quenched from 800, 1000, 1100 and 1200 °C, thermal analysis and dilatometry, two vertical sections for Ti-2.7 at.% Zr/Ti-25.3 at.% Al between 700 and 1750 °C and for Ti-2.7 at.% Zr/Ti-25.8 at.% Al, 2.4 at.% Zr between 500 and 1200 °C were determined.[73] Results of the former section were also published in (Ref 81) and in some more detail in (Ref 74). The latter section showing additional data for 700 °C was also published in (Ref 75). Though single data points fit well to data shown in Fig. 2 and 4, the general sequence of phase equilibria is not correct. While the phase equilibrium α(Ti,Zr) + β(Ti,Zr) + Ti_3Al is detected at 1000 °C in the former, i.e. more Zr lean section, it does not show up at this temperature in the latter, i.e. the more Zr rich one, which only shows the three-phase equilibrium at higher temperatures. According to Fig. 2, the three phase equilibrium should either be present in both sections or only in the more Zr-rich one, but not vice versa as shown in (Ref 73–75,81).

The α(Ti,Zr)/β(Ti,Zr) phase boundaries in the vertical section Ti-2.3 at.% Al/Ti-20 at.% Al, 2.3 at.% Zr were calculated in the temperature range 850-1000 °C and verified by analysing three alloys.[82] Comparison of the α(Ti,Zr)/β(Ti,Zr) phase boundaries at 1000 °C shows that they fit quite well to those shown in Fig. 2. The shift of the

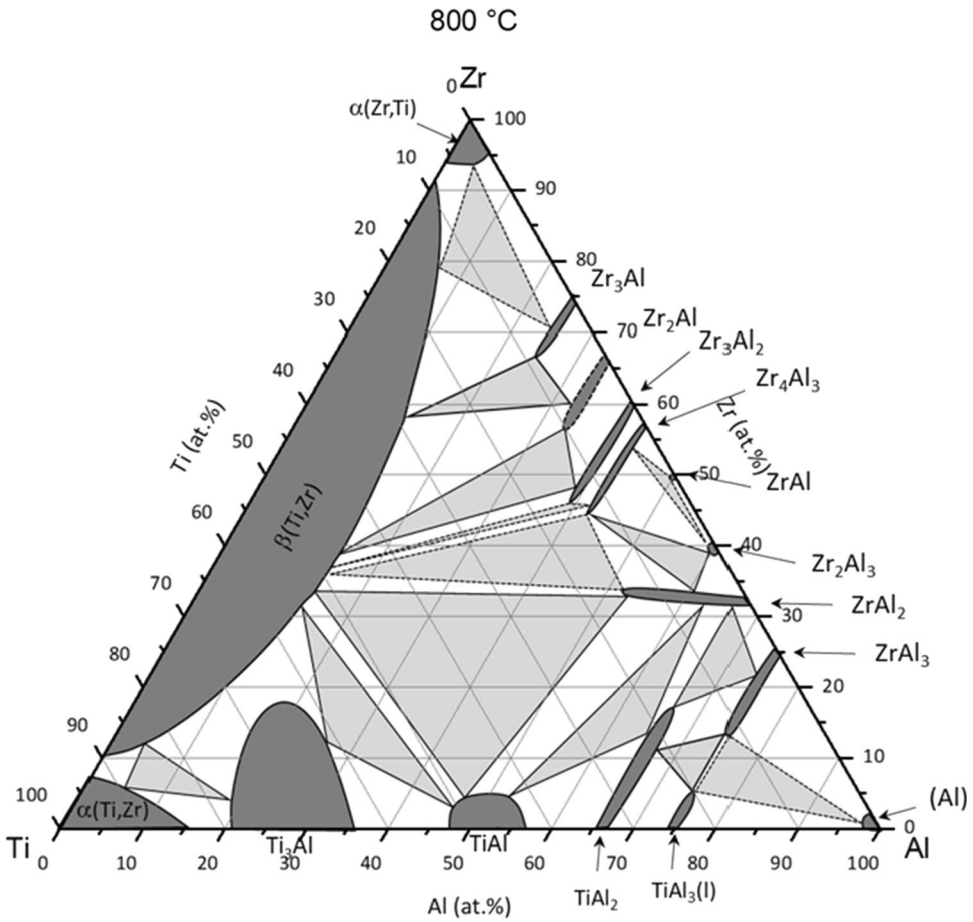

Fig. 4 Critically assessed isothermal section of the Al-Ti-Zr system at 800 °C

α(Ti,Zr)/α(Ti,Zr) + Ti_3Al phase boundary towards higher temperatures and lower Al contents with increasing Zr content is shown for the temperature range 500-700 °C in [2].

9 Modelling

Recently, CALPHAD-type and ab initio calculations were applied to establish isothermal sections at 800 and 1000 °C, partial isothermal sections of the Ti-corner at 1000, 1200 and 1300 °C and a vertical section along Ti-2.7 at.% Zr/Ti_3Al.[83] Thermodynamic parameters from binaries were extracted from (Ref 41, 34,84) for Ti-Al, Al-Zr, and Ti-Zr, respectively. Experimental data from[23–25,52,74] have been used to optimize thermodynamic parameters using the CALPHAD approach.

According to the modelling, the phase field of α(Ti,Zr) extends much further into the ternary system at 800 °C compared to (Ref 25), in line with the discussion of this section above. Also β(Ti,Zr) extends somewhat more into the ternary system at 800 °C, i.e. has a bit higher solid solubility for Al than shown in (Ref 25). The major difference between the isothermal sections for 800 °C, are that the experimental one shows phase equilibria between β(Ti,Zr) and $Zr(Al,Ti)_2$,[25] while the calculations show that TiAl should be in equilibrium with Zr_4Al_3.[83] Therefore, multiphase equilibria in a wide range of compositions in the two isotherms are quite different from each other as discussed in (Ref 83). Which of the two versions is correct cannot be decided on the existing evidence.

Modelled[83] and experimentally determined[24] isothermal sections at 1000 °C qualitatively match much better. Though, there are some differences in the solid solubility ranges of individual phases, most notably for Ti_3Al, which has less solid solubility for Zr according to the modelling. Otherwise, all multiphase equilibria in the experimental section are reproduced in the modelling. At higher temperatures there is quite some discrepancy at 1200 °C between the modelling[83] and experimental data in the Ti-corner,[23] while the match at 1300 °C is somewhat better. Calculated phase boundaries at 800 and 1000 °C of the vertical section[83] fit very well with those of the binary accepted here, with the sole exception for the α(Ti)/α(Ti) + Ti_3Al phase boundary at 800 °C, which according to Fig. 4 should be at a somewhat lower Al content.

A vertical section along (Ti,Zr)Al_3 has been calculated for 900-1100 °C.[85] In this section the two-phase field $D0_{22}$ + $D0_{23}$ is located much closer to the $TiAl_3$ ($D0_{22}$) side than in the experimentally determined section at 1000 °C (Fig. 1).[24] The relative stability of the $L1_2$, $D0_{22}$ and $D0_{23}$ structures along $TiAl_3$-$ZrAl_3$ was investigated at 0 K by calculating the enthalpy of formation using first principles calculations.[86] The results indicate that the $D0_{23}$ structure is the most stable along the complete section. While this finding agrees with experimental evidence for $ZrAl_3$, it is in contradiction for $TiAl_3$, where $D0_{23}$ is known to be the high-temperature polymorph while at lower temperatures $D0_{22}$ becomes stable. This discrepancy between ab initio calculations and experiments in case of $TiAl_3$ is well known and also discussed in (Ref 86).

Wang et al. (Ref 97) developed a thermodynamic description of the Al-Ti-Zr system, which was employed for reproducing the isothermal and vertical sections determined in (Refs 23–25, 74). In addition, the atomic mobility for β(Ti,Zr) has been assessed for the calculation of diffusion coefficients and diffusion paths determined in (Ref. 63) have been calculated. Also very recently, Abreu et al. (Ref 98) established the first liquidus projection of the system, based on detailed analysis of the microstructures of 27 as-cast alloys.

Acknowledgment The authors gratefully acknowledge funding from the Clean Sky 2 Joint Undertaking under the European Union's Horizon 2020 research and innovation program under Grant agreement No 820647.

Funding Open Access funding enabled and organized by Projekt DEAL.

References

1. I.I. Kornilov, Physical metallurgy of titanium (Metalovideniye Titana), in *5th Conference on Metallurgy, Physical Metallurgy, and Application of Titanium and its Alloys*, ed. by I.I. Kornilov (National Aeronautics and Space Administration, Moscow, 1963), pp. 1–351
2. F.A. Crossley, Effects of the Ternary Additions: O, Sn, Zr, Cb, Mo and V on the α/α + Ti_3Al Boundary of Ti-Al Base Alloys, *Trans. Metall. Soc. AIME*, 1969, **245**(9), p 1963–1968
3. G.K. Scarr, J.C. Williams, S. Ankem, and H.B. Bomberger, The effect of zirconium and oxygen on a_2 precipitation in titanium-aluminum alloys, in *5th Interntional Conference on Titanium*, eds. by G. Lütjering, U. Zwicker, W. Bunk (DGM, Munich, Germany, 1985), pp. 1475–1479
4. S. Tsunekawa and M.E. Fine, Lattice Parameters of $Al_3(Zr_xTi_{1-x})$ vs. x in Al-2 at.% (Ti + Zr) Alloys, *Scr. Metall.*, 1982, **16**, p 391–392
5. V.R. Parameswaran, J.R. Weertman, and M.E. Fine, Coarsening Behavior of $L1_2$ Phase in an Al-Zr-Ti Alloy, *Scr. Metall.*, 1989, **23**, p 147–150
6. K.M. Lee, J.H. Lee, and I.H. Moon, Effects of V and Zr Addition on Lattice Parameters of Al_3Ti Phase in Mechanically Alloyed Al-8 wt% Ti Alloys, *Scr. Metall. Mater.*, 1993, **29**, p 737–740
7. P. Málek, M. Janecek, B. Smola, P. Bartuska, and J. Plestil, Structure and Properties of Rapidly Solidified Al-Zr-Ti Alloys, *J. Mater. Sci.*, 2000, **35**, p 2625–2633
8. A.A. Abdel-Hamid, Crystallization of Complex Aluminide Compounds from Dilute Al-Ti Melts Containing One or Two Other Transition Metals of IVB to VIB Groups, *Z. Metallkd.*, 1990, **81**(8), p 601–605
9. B. Dubost, Applications industrielles et détermination des diagrammes d'équilibre de phases des alliages légers Progrès et perspectives (Industrial Applications and Determination of Equilibrium Phase Diagrams for Light Alloys Progress and Prospects), *Rev. Metall. (Paris)*, 1993, **90**(2), p 195–209 (in French)
10. L. Zhang, D.G. Eskin, and L. Katgerman, Influence of Ultrasonic Melt Treatment on the Formation of Primary Intermetallics and Related Grain Refinement in Aluminum Alloys, *J. Mater. Sci.*, 2011, **46**, p 5252–5259
11. G.J. Fan, X.P. Song, M.X. Quan, and Z.Q. Hu, Mechanical Alloying and Thermal Stability of $Al_{67}Ti_{25}M_8$ (M = Cr, Zr, Cu), *Mater. Sci. Eng., A*, 1997, **231**, p 111–116
12. M.V. Karpets, Y.V. Milman, O.M. Barabash, N.P. Korzhova, O.N. Senkov, D.B. Miracle, T.N. Legkaya, and I.V. Voskoboynik, The Influence of Zr Alloying on the Structure and Properties of Al_3Ti, *Intermetallics*, 2003, **11**, p 241–249
13. S.S. Nayak, S.K. Pabi, and B.S. Murty, High Strength Nanocrystalline L12-Al3(Ti, Zr) Intermetallic Synthesized by Mechanical Alloying, *Intermetallics*, 2007, **15**, p 26–33
14. K.E. Knipling, D.C. Dunand, and D.N. Seidman, Precipitation Evolution in Al–Zr and Al–Zr–Ti Alloys During Aging at 450–600°C, *Acta Mater.*, 2008, **56**, p 1182–1195
15. E.A. Popova, A.B. Shubin, P.V. Kotenkov, E.A. Pastukhov, L.E. Bodrova, and O.M. Fedorova, Al–Ti–Zr Master Alloys: Structure Formation, *Russ. Metall. (Engl. Transl.)*, 2012, **2012**(5), p 357–361
16. E.A. Popova, P.V. Kotenkov, E.A. Pastukhov, and A.B. Shubin, Master Alloys Al–Sc–Zr, Al–Sc–Ti, and Al–Ti–Zr: Their Manufacture, Composition, and Structure, *Russ. Metall. (Engl. Transl.)*, 2013, **13**(8), p 590–594
17. P. Kotenkov, E. Popova, and I. Gilev, Formation of stable and metastable aluminides in Al–Zr–Ti, Al–Ti–Nb alloys, in *Physics, Technologies and Innovation (PTI-2018): Proceedings of the V International Young Researchers' Conference*, eds. by V.A. Volkovich, S.V. Zvonarev, I.V. Kashin, E.D. Narkhov (Ekaterinburg, Russia, 2018), p. 020046
18. S.V. Spragins, J.R. Myers, and R.K. Saxer, Influence of Zirconium Additions on the Epsilon Phase of the Titanium-Aluminium System, *Nature Lett.*, 1965, **4993**(10), p 183–184
19. K. Hashimoto, H. Doi, K. Kasahara, T. Tsujimoto, and T. Suzuki, Effects of Third Elements on the Structures of TiAl-Based

Alloys, *Nippon Kinzoku Gakkaishi (J. Jpn. Inst. Met.)*, 1988, **52**(8), p 816–825 (in Japanese)
20. H. Doi, K. Hashimoto, K. Kasahara, and T. Tsujimoto, Site Determination of Third Elements in TiAl Compound by X-ray Diffractometry, *Mater. Trans., JIM*, 1990, **31**(11), p 975–982
21. X.F. Chen, R.D. Reviere, B.F. Oliver, and C.R. Brooks, The Site Location of Zr Atoms Dissolved in TiAI, *Scr. Metall. Mater.*, 1992, **27**, p 45–49
22. C.T. Forwood, M.A. Gibson, P.R. Miller, C.J. Rossouw, and A.J. Morton, Alloying effects and deformation processes in duplex g-TiAl alloys, in *Structural Intermetallics 1997*, eds. by M.V. Nathal, R. Darolia, C.T. Liu, P.L. Martin, D.B. Miracle, R. Wagner, M. Yamaguchi (Seven Springs, PA, TMS, Warrendale, PA, 1997), pp. 545–554
23. R. Kainuma, Y. Fujita, H. Mitsui, I. Ohnuma, and K. Ishida, Phase Equilibria Among a (hcp), b (bcc) and g (L_{10}) Phases in Ti-Al Base Ternary Alloys, *Intermetallics*, 2000, **8**, p 855–867
24. F. Yang, F.H. Xiao, S.G. Liu, S.S. Dong, L.H. Huang, Q. Chen, G.M. Cai, H.S. Liu, and Z.P. Jin, Isothermal Section of Al–Ti–Zr Ternary System at 1273 K, *J. Alloys Compd.*, 2014, **585**, p 325–330
25. K.L. Lü, F. Yang, Z.Y. Xie, H.S. Liu, G.M. Cai, and Z.P. Jin, Isothermal Section of Al − Ti − Zr Ternary System at 1073 K, *Trans. Nonferrous Met. Soc. China*, 2016, **26**, p 3052–3058
26. J.L. Murray, Al-Ti system, *Phase Diagrams of Binary Titanium Alloys*, J.L. Murray, Ed., ASM, Washington, DC, 1987, p 12–24
27. J.C. Schuster and M. Palm, Reassessment of the Binary Aluminium-Titanium Phase Diagram, *J. Phase Equilib. Diffus.*, 2006, **27**(3), p 255–277
28. D.H. Troup, *An Investigation of the Gamma Phase of the Binary Titanium-Aluminum Alloy With Zirconium Additions*, M.Sc., Air University, Islamabad, 1962
29. I. Ansara, B. Grieb, and B. Legendre, *Al-Ti-Zr Ternary Phase Diagram Evaluation*, MSI, Materials Science International Services GmbH, Stuttgart, 1993
30. L. Tretyachenko, *Al-Ti-Zr Ternary Phase Diagram Evaluation*, MSI, Materials Science International Services GmbH, Stuttgart, 2004
31. J. Schuster, *Al-Zr Binary Phase Diagram Evaluation*, MSI, Materials Science International Services GmbH, Stuttgart, 2004
32. J. Murray, A. Peruzzi, and J.P. Abriata, The AI-Zr (Aluminum-Zirconium) System, *J. Phase Equilib.*, 1992, **13**(3), p 277–291
33. H. Okamoto, Al-Zr, *J. Phase Equilib.*, 2002, **23**(5), p 455–456
34. T. Wang, Z.P. Jin, and J.C. Zhao, Thermodynamic Assessment of the Al-Zr Binary System, *J. Phase Equilib. Diffus.*, 2001, **22**(5), p 544–551
35. E. Fischer and C. Colinet, An Updated Thermodynamic Modeling of the Al-Zr System, *J. Phase Equilib. Diffus.*, 2015, **36**(5), p 404–413
36. R. Tamim and K. Mahdouk, Thermodynamic Reassessment of the Al–Zr Binary System, *J. Therm. Anal. Calorim.*, 2018, **131**, p 1187–1200
37. A. Janghorban, A. Antoni-Zdziobek, M. Lomello-Tafin, C. Antion, T. Mazingue, and A. Pisch, Phase Equilibria in the Aluminium-Rich Side of the Al–Zr System, *J. Therm. Anal. Calorim.*, 2013, **114**, p 1015–1020
38. A. Peruzzi, Reinvestigation of the Zr-Rich End of the Zr-Al Equilibrium Phase Diagram, *J. Nucl. Mater.*, 1992, **186**, p 89–99
39. A. Malfliet, A. Kozlov, and N. Lebrun, *Ti-Zr Binary Phase Diagram Evaluation*, MSI, Materials Science International, Stuttgart, 2015
40. B. Batalu, G. Cosmeleata, and A. Aloman, Critical Analysis of the Ti-Al Phase Diagrams, *U.P.B. Sci. Bull., Series B*, 2006, **68**(4), p 77–90
41. V.T. Witusiewicz, A.A. Bondar, U. Hecht, S. Rex, and T.Y. Velikanova, The Al-B-Nb-Ti System: III, Thermodynamic Re-evaluation of the Constituent Binary System Al-Ti, *J. Alloys Compd.*, 2008, **465**(1–2), p 64–77
42. M. Palm, *Al-Ti Binary Phase Diagram Evaluation*, MSI, Materials Science International, Stuttgart, 2020
43. H. Wang, R.C. Reed, J.-C. Gebelin, and N. Warnken, On the Modelling of the Point Defects in the Ordered B2 Phase of the Ti–Al System: Combining CALPHAD with First-Principles Calculations, *CALPHAD: Comput. Coupling Phase Diagr. Thermochem.*, 2012, **39**, p 21–26
44. J.L. Murray, Calculation of the Titanium-Aluminum Phase Diagram, *Metall. Trans.*, 1988, **19A**(2), p 243–247
45. U.R. Kattner, J.-C. Lin, and Y.A. Chang, Thermodynamic Assessment and Calculation of the Ti-Al System, *Metall. Trans.*, 1992, **23A**(8), p 2081–2090
46. N. Saunders, in *System Al-Ti, COST507: Thermochemical Database for Light Metal Alloys*, ed. by I. Ansara (ECSC-EEC-EAEC, Brussles and Luxembourg, 1995), pp. 52–56
47. F. Zhang, S.L. Chen, Y.A. Chang, and U.R. Kattner, A Thermodynamic Description of the Ti-Al System, *Intermetallics*, 1997, **5**, p 471–482
48. I. Ohnuma, Y. Fujita, H. Mitsui, K. Ishikawa, R. Kainuma, and K. Ishida, Phase Equilibria in the Ti-Al Binary System, *Acta Mater.*, 2000, **48**, p 3113–3123
49. C.M. Fang and Z. Fan, An Ab Initio Study on Stacking and Stability of $TiAl_3$ Phases, *Comput. Mater. Sci.*, 2018, **153**, p 309–314
50. E. Illeková, P. Švec, and D. Janičkovič, Influence of the Processing on the Ordering Process in the Al-Ti Binary System with Composition Close to Al_3Ti, *J. Phys: Conf. Ser.*, 2009, **144**, p 012111
51. D. Sornadurai, B. Panigrahi, and V.S. Sastry, Ramani, Crystal Structure and X-ray Powder Diffraction Pattern of Ti_2ZrAI, *Powder Diffr.*, 2000, **15**(3), p 189–190
52. M. Premkumar, K.S. Prasad, and A.K. Singh, Structure and Stability of the B2 Phase in Ti–25Al–25Zr Alloy, *Intermetallics*, 2009, **17**, p 142–145
53. A. Pathak and A.K. Singh, A First Principles Study of Structural and Mechanical Properties of Ti_2AlZr Intermetallic, *Intermetallics*, 2015, **63**, p 37–44
54. D. Sornadurai, V.S. Sastry, V.T. Paul, R. Flemming, F. Jose, R. Ramaseshan, and S. Dash, Microstructure, Crystal Structure and Mechanical Properties of the New Ternary Intermetallic Alloy Phase Zr_2TiAl, *Intermetallics*, 2012, **24**, p 89–94
55. I.I. Kornilov, T.T. Nartova, and M.M. Savel'yeva, Phase equilibrium of alloys of the section Ti_3Al-Zr of the ternary system Ti-Al-Zr, *Metallovedeniye Titana*, I.I. Kornilov, Ed., Nauka, Moscow, 1964, p 53–57
56. X.J. Jiang, Y.K. Zhou, Z.H. Feng, C.Q. Xia, C.L. Tan, S.X. Liang, X.Y. Zhang, M.Z. Ma, and R.P. Liu, Influence of Zr Content on β-Phase Stability in α-Type Ti–Al Alloys, *Mat. Sci. Eng.*, 2015, **A639**, p 407–411
57. Y. Miyajima, K. Ishikawa, and K. Aoki, Hydrogen-Induced Amorphization in Ti–Al–Zr Compounds with $D0_{19}$, B2 and FCC Structures, *Mater. Trans.*, 2002, **43**(5), p 1085–1088
58. M. Premkumar and A.K. Singh, Deformation Behavior of an Ordered B2 Phase in Ti–25Al–25Zr Alloy, *Intermetallics*, 2010, **18**, p 199–201
59. G.N. Muradyan, S.K. Dolukhanyan, A.G. Aleksanyan, O.P. Ter-Galstyan, and N.L. Mnatsakanyan, Regularities and Mechanism of Formation of Aluminides in the TiH_2-ZrH_2-Al System, *Russ. J. Phys. Chem. B*, 2019, **13**(1), p 86–95
60. C. Ravi, P. Vajeeston, S. Mathijaya, and R. Asokamani, Electronic Structure, Phase Stability, and Cohesive Properties of Ti_2XAl (X = Nb, V, Zr), *Phys. Rev. B*, 1999, **60**(23), p 15683–15690

61. C. Ravi and R. Asokamani, Site Preference of Zr in Ti_3Al and Phase Stability of Ti_2ZrAl, *Bull. Mater. Sci.*, 2003, **26**(1), p 97–103
62. P. Modak, L.M. Ramaniah, and A.K. Singh, Structure of the B2 Phase in the Ti–25Al–25Zr Alloy: A Density Functional Study, *J. Phys.: Condens. Matter*, 2010, **22**, p 345502
63. F. Fan, Y. Gu, G. Xu, H. Chang, and Y. Cui, Diffusion Research in BCC Ti-Al-Zr Ternary Alloys, *J. Phase Equilib. Diffus.*, 2019, **40**, p 686–696
64. I.I. Kornilov and N.G. Boriskina, Study of the phase structure of the alloys of the system Ti-Al-Zr along the Ti_3Al-Zr section, *Metallovedeniye Titana*, I.I. Kornilov, Ed., Nauka, Moscow, 1964, p 58–66
65. Y.L. Hao, D.S. Xu, Y.Y. Cui, R. Yang, and D. Li, The Site Occupancies of Alloying Elements in TiAl and Ti_3Al Alloys, *Acta Mater.*, 1999, **47**(4), p 1129–1139
66. R. Yang, Y. Hao, Y. Song, and Z.-X. Guo, Site Occupancy of Alloying Additions in Titanium Aluminides and Its Application to Phase Equilibrium Evaluation, *Z. Metallkd.*, 2000, **91**(4), p 296–301
67. A. Prince, *Alloy Phase Equilibria*, Elsevier, Amsterdam, 1966
68. F. Stein, G. Sauthoff, and M. Palm, Phases and Phase Equilibria in the Fe-Al-Zr System, *Z. Metallkd.*, 2004, **96**(6), p 469–485
69. J.C. Schuster, J. Bauer, and J. Debuigne, Investigation of Phase Equilibria Related to Fusion Reactor Materials: I. The Ternary System Zr-AI-N, *J. Nucl. Mater.*, 1983, **116**(2–3), p 131–135
70. D. Tanda, T. Tanabe, R. Tamura, and S. Takeuchi, Synthesis of Ternary $L1_0$ Compounds of Ti–Al–Zr System and Their Mechanical Properties, *Mat. Sci. Eng.*, 2004, **A387–389**, p 991–995
71. K. Kasahara, K. Hashimoto, H. Doi, and T. Tsujimoto, Crystal Structure and Hardness of TiAl Phase Containing Zirconium, *Nippon Kinzoku Gakkaishi (Journal of the japan institute of metals)*, 1987, **51**(4), p 278–284, in Japanese
72. Y.N. Pylaeva and M.A. Volkova, Study of the alloys of the ternary system Ti-Al-Zr, *Metallovedeniye Titana*, I.I. Kornilov, Ed., Nauka, Moscow, 1964, p 38–42
73. N.I. Shirokova and T.T. Nartova, Investigation of the phase equilibrium and properties of alloys of the titanium corner of the system Ti-Zr-Al, *Titanovyye Splavy dlya Novoy Tekhniki*, N.P. Sazhin, Ed., Nauka, Moscow, 1968, p 101–106
74. N.I. Shirokova, T.T. Nartova, and I.I. Kornilov, Investigation of the Phase Equilibrium and Properties of Ti-Zr-Al Alloys, *Izvestia Akademii nauk SSSR. Metally*, 1968, **1968**(4), p 183–187 (in Russian)
75. T.T. Nartova and N.I. Shirokova, Phase equilibria and heat resistance of Ti-Zr-Al alloys, *Izvestia Akademii nauk SSSR. Metally*, 1970, **1970**(3), p 194–198, in Russian
76. Y.N. Borisova and I.I. Shashenkova, Study of the properties of alloys of the sytems Ti-Zr and Ti-Zr-Al, *Titanovyye Splavy dlya Novoy Tekhniki*, N.P. Sazhin, Ed., Nauka, Moscow, 1970, p 202–207
77. D. Xu, W. Long, and X. Zhou, Microstructure and Corrosion Resistance of Al_3(Zr, Ti)/Al Composite Prepared by Powder Metallurgy, *Adv. Compos. Lett.*, 2020, **29**, p 1–9
78. D.L.Y. Li and X. Wan, On the Thermal Stability of Ti Alloys, *Acta Metall. Sinica*, 1984, **20**(A), p 375–383
79. D.R. Sandlin and H.A. Klung, *A Phase Study of a Selected Portion of the Ti-Al-Zr Ternary System Inclucing Lattice Parameter Determination for the Ti-Al Gamma Phase*, Air University, Islamabad, 1961
80. T.B. Massalski, *Binary Alloy Phase Diagrams*, 2nd ed., ASM International, Metals Park, OH, 1990
81. N.I. Shirokova, T.T. Nartova, and I.I. Kornilov, Investigation of the Phase Equilibrium and Properties of Ti-Zr-Al Alloys, *Russ. Metall. (Engl. Transl.)*, 1968, **1968**(4), p 115–117
82. J.P. Gros, I. Ansara, and M. Allibert, Prediction of α/β equilibria in titanium-based alloys containing Al, Mo, Zr, Cr (Part II), in *6th World Conference on Titanium*, eds. by P. Lacombe, R. Tricot, G. Béranger (Les Editions de Physique, Cannes, France, 1988) Les Ulis Cedex, France, pp. 1559–1564
83. Z.X. Deng, D.P. Zhao, Y.Y. Huang, L.L. Chen, H. Zou, Y. Jiang, and K. Chang, Ab Initio and CALPHAD-Type Thermodynamic Investigation of the Ti–Al–Zr System, *J. Min. Metall., Sect. B*, 2019, **55**(3), p 427–437
84. H.K.C. Kumar, P. Wollants, and L. Delaey, Thermodynamic Assessment of the Ti-Zr System and Calculation of the Nb-Ti-Zr Phase Diagram, *J. Alloys Compd.*, 1994, **202**, p 121–127
85. S.I. Park, S.Z. Han, S.K. Choi, and H.M. Lee, Phase Equilibria of Al3(Ti, V, Zr) Intermetallic System, *Scr. Mater.*, 1996, **34**(11), p 1697–1704
86. G. Ghosh, S. Vaynman, M. Asta, and M.E. Fine, Stability and Elastic Properties of L12-(Al, Cu)3(Ti, Zr) Phases: Ab Initio Calculations and Experiments, *Intermetallics*, 2007, **15**, p 44–54
87. M.J. Blackburn, The Ordering Transformation in Titanium: Aluminum Alloys Containing up to 25 at pct Al, *Trans. Metall. Soc. AIME*, 1967, **239**(8), p 1200–1208
88. J. Braun, M. Ellner, and B. Predel, Experimental Investigation of the Structure and Stability of the Phase TiAl, *Z. Metallkd.*, 1995, **86**(12), p 870–876
89. H. Mabuchi, T. Asai, and Y. Nakayama, Aluminide Coatings on TiAl Compound, *Scr. Metall.*, 1989, **23**, p 685–689
90. J.C.I. Schuster, Phases and Phase Relations in the Partial System $TiAl_3$-TiAl, *Z. Metallkd.*, 1990, **81**(6), p 389–396
91. A.S. Raman, The Constitution of Some Alloy Series Related to $TiAl_3$. II. Investigations in Some T-Al-Si and $T^{4\ldots6}$-In Systems, *Z. Metallkd.*, 1965, **56**(1), p 44–52
92. R. Miida, One Dimensional Antiphase Domain Structures in the Aluminum-Rich Al-Ti Alloys, *Jpn. J. Appl. Phys.*, 1986, **25**(12), p 1815–1824
93. F.J.J. van Loo and G.D. Rieck, Diffusion in the Titanium-Aluminium System—I. Interdiffusion Between Solid Al and Ti or Ti-Al Alloys, *Acta Metall.*, 1973, **21**(1), p 61–71
94. J. Braun and M. Ellner, Phase Equilibria Investigations on the Aluminium-Rich Part of the Binary System Ti-Al, *Metall. Mater. Trans. A*, 2001, **32A**(5), p 1037–1047
95. M. Pötzschke and K. Schubert, Zum Aufbau einiger zu T^4-B^3 homologer und quasihomologer. Systeme II, Die Systeme Ti-Al, Zr-Al, Hf-Al, Mo-Al und einige ternäre Systeme, *Z. Metallkd.*, 1962, **53**(8), p 548–561 (in German)
96. H. Nowotny, H. Auer-Welsbach, J. Bruss, and A. Kohl, Ein Beitrag zur Mn_5Si_3-Struktur (D 8_8-Typ). Monatsh, *Chem. Verw. Teile Anderer Wiss. Chem. Mon.*, 1959, **90**, p 15–23
97. J. Wang, W. Zheng, G. Xu, X. Zeng, and Y. Cui, Thermodynamic assessment of the Ti–Al–Zr system and atomic mobility of its bcc phase, *CALPHAD*, 2020, **70**, p 101801
98. D.A. Abreu, A.A.A.P. Silva, J.C.P. Santos, D.F. Barros, C.S. Barros, N. Chaia, C.A. Nunes, and G.C. Coelho, Liquidus projection of the Al-Ti-Zr system, *J. Alloys Compd.*, 2020, **849**, p 156463